Temporal behavior of bidimensional photorefractive bright spatial solitons

N. Fressengeas,[1,2] J. Maufoy,[1] and G. Kugel[2]

[1]*Service Electronique, Supélec, 2 rue Edouard Belin, 57078 Metz Cedex 3, France*

[2]*Laboratoire Matériaux pour l'Optique à Propriétés Spécifiques, Centre Lorrain d'Optique et d'Electronique des Solides,
Université de Metz-Supélec, 2 rue Edouard Belin, 57078 Metz Cedex 3, France*

The time behavior of bright spatial solitons in biased photorefractive media is investigated within the framework of a bidimensional band transport model. Biasing the photorefractive media requires an externally applied electric field or the presence of a photovoltaic effect. These two basically different phenomena are shown to be equivalent and additive. The mechanism of space-charge field buildup is analytically expressed, leading to a time-dependent wave propagation equation in generic photorefractive media. The temporal behavior of the soliton solutions to this equation is investigated. It shows the evolution of the soliton beam from the time the external electric field is applied to the final steady-state soliton. On the way, the so-called quasisteady soliton is retrieved, along with its properties. Furthermore, the photovoltaic soliton is described by the wave propagation equation: its behavior is the same as that of the steady-state soliton, the transient states included. Finally, low-power photorefractive bright spatial solitons are generated in a $Bi_{12}TiO_{20}$ crystal with a He-Ne laser and their temporal behavior is investigated, thus providing an experimental validation of our theoretical considerations. [S1063-651X(96)06912-7]

PACS number(s): 42.65.Tg,42.65.Sf,42.65.Hw,42.65.Jx

INTRODUCTION

The photorefractive effect is the result of a complex combination of various physical phenomena. The most commonly studied photorefractive effect stems from charge transport and trapping, which induce a space-charge electric field and thus an index variation. The propagation of a single light beam through such a medium has been the focus of many recent studies. In particular, bright spatial solitons have been predicted [1–4], leading to the observation of photorefractive self-focusing effects [5] and of photorefractive spatial solitons [6–9]. These phenomena occur only if the photorefractive material is properly biased by an externally applied electric field or by the presence of a photovoltaic nonlinearity.

The self-focusing process has been found to lead to three different types of bright spatial soliton: the quasi-steady-state soliton [1,2,10], which has a limited lifetime and does not depend on light intensity as long as it is much larger than the dark irradiance; the screening soliton [7,11], which occurs at steady state and is due to the partial screening of the externally applied electric field; and the photovoltaic soliton [8,12], which can be obtained without any external electric field, the photorefractive material being biased by the presence of the photovoltaic effect.

The ability to generate spatial solitons at optical powers in the range of the mW/cm^2 level seems promising for applications such as all-optical routing or beam reshaping. The major drawback of the photorefractive effect is, however, its low response time when compared to that of the Kerr effect, which has been previously found to allow spatial soliton propagation as well [13]. That is the reason why the temporal behavior of the photorefractive soliton beam has to be studied carefully. A nonstationary bidimensional model leading to numerical simulations has been developed recently [14,15]. However, it does not provide an explicit wave propagation equation. Therefore, in order to achieve a further understanding of the phenomena involved, a simpler model that can lead to a time-dependent wave propagation equation has to be developed. In this paper, such a theory is proposed and it is suggested that linking the three types of soliton through one partial differential equation depending on the time is possible, within the framework of a bidimensional band-transport model. The time evolution of the photorefractive soliton profile is numerically evaluated and the key role played by the saturation process is shown. Consistent experimental evidence on a $Bi_{12}TiO_{20}$ crystal is then provided.

I. THEORETICAL BASIS AND APPROXIMATIONS

In a crystal whose dimensions are considered to be infinite and under the standard assumption of slow variation along the transversal direction x, the band-transport model reduced to one dimension can lead to an analytical expression of the space-charge field. To achieve it, further approximations concerning charge-carrier densities are needed and detailed below. A wave propagation equation can then be derived.

The band-transport model is summarized in a very general manner by the set of equations (1) developed by Kukhtarev *et al.* [16],

$$\frac{\partial}{\partial t}N_D^+ = (\beta + sI_{em})(N_D - N_D^+) - \xi n_e N_D^+, \tag{1a}$$

$$\nabla \cdot (\varepsilon_0 \hat{\varepsilon}_r \mathbf{E}) = \rho, \tag{1b}$$

$$\frac{\partial}{\partial t}\rho + \nabla \cdot \mathbf{J} = 0, \tag{1c}$$

$$\rho = e(N_D^+ - N_A - n_e), \tag{1d}$$

$$\mathbf{J} = e\mu n_e \mathbf{E} + \mu \kappa_B T \nabla \mathbf{n_e} + \beta_{ph}(N_D - N_D^+)\mathbf{c}I_{em}. \tag{1e}$$

The densities N_D^+ and n_e of ionized donors and electrons are functions of space and time, as well as the charge and current densities ρ and $\mathbf{J}$, the electric field $\mathbf{E}$, and the beam local power density I_{em}. N_D and N_A are the densities of donors and acceptors, β and s are the thermal and photoexcitation coefficients, ξ is the recombination constant, e is the elementary charge, ε_0 is the electric permeability of the vacuum, $\hat{\varepsilon}_r$ is the static dielectric tensor, μ is the electron mobility, κ_B is the Boltzmann constant, T is the temperature, and β_{ph} is the component of the photovoltaic tensor along the ferroelectric $\mathbf{c}$ axis, the other components being neglected. In the following, the x direction is along the $\mathbf{c}$ axis.

For the sake of simplicity, we will consider an electromagnetic wave that propagates along z and is allowed to diffract in only one direction x along the ferroelectric $\mathbf{c}$ axis. Under this assumption, the current density $\mathbf{J}$ expressed in (1e) is then allowed to be directed in only one direction. This model does not allow $\mathbf{J}$ to do vortices like in Ref. [14]. Nevertheless, although this model forces the current distribution to be along the x direction, the current loop can be closed if the crystal faces are linked by a conductor, which is the case if an electric field is applied.

Under this assumption the set of equations (1) reduces to the set of equations

$$\frac{\partial}{\partial t}N_D^+ = (\beta + sI_{\mathrm{em}})(N_D - N_D^+) - \xi n_e N_D^+, \qquad (2a)$$

$$\frac{\partial}{\partial x}(\varepsilon_0 \varepsilon_r E) = \rho, \qquad (2b)$$

$$\frac{\partial J}{\partial x} + \frac{\partial \rho}{\partial t} = 0, \qquad (2c)$$

$$\rho = e(N_D^+ - N_A - n_e), \qquad (2d)$$

$$J = e\mu n_e E + \mu \kappa_B T \frac{\partial n_e}{\partial x} + \beta_{\mathrm{ph}}(N_D - N_D^+)I_{\mathrm{em}}. \qquad (2e)$$

ε_r is the component of the static dielectric tensor along the x direction.

In typical photorefractive media and provided light intensity is not too high, the density of free electrons compared to that of donors and acceptors can be neglected: $N_A \gg n_e$. This implies that the densities of ionized donors and acceptors are quasiequal, which, along with the slowly varying assumption, implies that

$$eN_A \gg \varepsilon_0 \varepsilon_r \frac{\partial E}{\partial x}.$$

The latter approximation is akin to writing that the Debye wave number (see Sec. II A for a precise definition) is much larger than unity [14].

II. STEADY-STATE STUDY

A. Further approximations and a space-charge field general expression

Under steady-state conditions and under the assumptions stated above, the set of equations (2) can be reduced to a single differential equation (3) linking the space-charge field E, the total light intensity I, and their spatial derivatives,

$$\frac{n_0}{I_0}[E_{\mathrm{ph}}e\mu I' + e\mu(IE)' + \kappa_B T\mu I''] - \beta_{\mathrm{ph}}\frac{\varepsilon_0 \varepsilon_r}{e}(I - I_d)E''$$

$$- \frac{N_D se}{\xi N_A k_D^2}\left[\frac{e}{\kappa_B T}IEE'' + 2I'E'' + IE'''\right] = 0. \qquad (3)$$

Here n_0 is the free-electron density generated by an arbitrary uniform illumination I_0:

$$\frac{n_0}{I_0} = \frac{s(N_D - N_A)}{\xi N_A}.$$

$I_d = \beta/s$ is the dark irradiance, $k_D = \sqrt{e^2 N_A/\kappa_B T\varepsilon_0 \varepsilon_r}$ is the Debye wave number, and $E_{\mathrm{ph}} = \beta_{\mathrm{ph}}\xi N_A/e\mu s$ is the electric field characteristic of the photovoltaic effect. The quantity $I = I_{\mathrm{em}} + I_d$ is the generalized light intensity, taking in account both thermal and photoexcitation, and is thus a function of the transverse spatial coordinate x.

Assuming that the recombination rate is high enough so that $N_D sI \ll \xi N_A^2$ [17] and considering that $k_D \gg 1$, the last term of Eq. (3) compared to the first two can be neglected. Furthermore, if typical quantitative values are considered for the remaining two terms, the second one can be neglected by comparison to the first one. Therefore Eq. (3) is reduced to

$$e\mu[E_{\mathrm{ph}}I' + (IE)'] + \kappa_B T\mu I'' = 0. \qquad (4)$$

Introducing a generalized space-charge electric field $E_\tau = E + E_{\mathrm{ph}}$, it is straightforward to show that Eq. (4) can be reduced to

$$(IE_\tau)' + \frac{\kappa_B T}{e}I'' = 0. \qquad (5)$$

This latter differential equation links two functions of the space variable: I and E_τ. It can, however, be integrated so as to give an expression of E_τ as a function if I.

B. Boundary conditions and solution

Solving Eq. (5) requires initial conditions on both E and I. The material being assumed infinite in the x direction, the beam influence can be considered to be limited to its vicinity: all the derivatives of I are considered null far from the beam. However, only the hypothesis $\lim_{x\to\infty}I'(x) = 0$ is strictly needed. Therefore, the useful part of the beam I_{em} vanishes at infinity: $\lim_{x\to\infty}I = I_d$. Furthermore, the electric field far from the beam remains quasiunaffected: $\lim_{x\to\infty}E = E_{\mathrm{ext}} \Leftrightarrow \lim_{x\to\infty}E_\tau = E_{\mathrm{ext}} + E_{\mathrm{ph}}$, E_{ext} being simply the voltage applied to the crystal, divided by the crystal width. Under those conditions, the generalized electric field E_τ can be expressed as

$$E_\tau = \frac{(E_{\mathrm{ext}} + E_{\mathrm{ph}})I_d}{I} - \frac{\kappa_B T}{e}\frac{I'}{I}. \qquad (6)$$

Equation (6) shows the similar role played by the external electric field E_{ext} and by the photovoltaic effect whose influence is shown by E_{ph}. This symmetry between these basi-

cally different two physical processes will be seen throughout the paper to the final wave propagation equation (WPE).

C. Wave propagation equation

1. General expression of the WPE

The propagation of an electromagnetic wave in a medium with a low index modulation δn and negligible absorption can be expressed as

$$\left(\frac{\partial}{\partial z} - \frac{i}{2k}\frac{\partial^2}{\partial x^2}\right)\mathcal{E} = \frac{ik}{n}\,\delta n\mathcal{E}. \qquad (7)$$

z is the propagation direction, x is the direction in which the beam is allowed to diffract, $\mathcal{E}$ is the amplitude of the beam electric field, k is the wave vector, and n is the base refractive index.

Via the Pockels effect (or electro-optic effect), the index modulation is directly proportional to the space-charge electric field, via the effective electro-optic coefficient r_{eff}:

$$\delta n = -\tfrac{1}{2}n^3 r_{\text{eff}}E. \qquad (8)$$

If we leave out the constant refractive index change induced by I_d, a new wave propagation equation can be derived from Eqs. (6)–(8),

$$i\frac{\partial U}{\partial Z} + \frac{1}{2}\frac{\partial^2 U}{\partial X^2} - \left(N^2 - D\frac{\partial|U|^2}{\partial X}\right)\frac{U}{|U|^2+1} = 0, \qquad (9)$$

with $U = \mathcal{E}/\sqrt{I_d}$, $X = x/X_0$, and $Z = z/kX_0^2$, where X_0 is an arbitrary length.

N^2 is characteristic of the quasilocal mechanisms of nonlinearity and is due to drift and photovoltaic mechanisms of transport:

$$N^2 = \frac{k^2 n^2 r_{\text{eff}} X_0^2 (E_{\text{ext}} + E_{\text{ph}})}{2}. \qquad (10)$$

The drift mechanism of transport is due to the externally applied electric field E_{ext}, while the photovoltaic effect is represented in Eq. (10) by E_{ph}. Equation (10) again shows how and why these two basically different phenomena can be considered similar. Their influence on the wave propagation is shown to be additive.

An equation of the same type as (9) has been found to exhibit bright soliton solutions [18]. These particular soliton solutions can, however, only be achieved if N^2 is positive, which physically means that the nonlinearity is such that refractive index diminishes if the local optical intensity rises [11,18]. If N^2 happens to be negative, the beam is then self-defocused.

The quantity D is characteristic of the diffusion mechanism of transport and is expressed by

$$D = \frac{k^2 n^2 r_{\text{eff}} X_0 \kappa_B T}{2e}. \qquad (11)$$

The diffusion mechanism of transport is essentially dependent on the crystal type and on the charge-density gradient. It has been numerically found to induce self-deflection of the

soliton beam [19]: strictly speaking, soliton beams can be achieved only if this term is neglected.

The physical meaning of the arbitrary length X_0, introduced to render Eq. (9) dimensionless, cannot be defined precisely here. Its real significance can only be inferred from the mathematical solution of Eq. (9). However, well-known hyperbolic secant solutions of the similar nonlinear Schrödinger equation (see Sec. II C 3 below) suggest that X_0 is closely related to the beam half-width.

2. Simplification of the WPE by neglecting diffusion-related terms

As suggested by Ref. [18], an interesting approach to Eq. (9) is the case when the diffusion mechanism of transport plays no significant role: $N^2 \gg D\partial|U|^2/\partial X$. This is true if the drift mechanisms due to the external field and to the photovoltaic effect are strong enough: $E_{\text{ext}} + E_{\text{ph}} \gg (\kappa_B T/e)(1/I_d)(\partial I/\partial x)$. In that particular case, the wave propagation equation (9) reduces to

$$i\frac{\partial U}{\partial Z} + \frac{1}{2}\frac{\partial^2 U}{\partial X^2} - N^2\frac{U}{|U|^2+1} = 0. \qquad (12)$$

Equation (12) is a generalized nonlinear Schrödinger equation of the form

$$i\frac{\partial U}{\partial Z} + \frac{1}{2}\frac{\partial^2 U}{\partial X^2} + f(|U|^2)U = 0.$$

It is now known to exhibit soliton solutions [18].

3. Case of intense dark irradiance

Both Eqs. (9) and (12) clearly show the key role that the dark irradiance plays in the photorefractive self-focusing process. Since the dark irradiance models the thermal charge carrier generation, it is possible to artificially increase and control it by shedding a background uniform light upon the whole crystal [7].

In this condition, it is meaningful to consider the case when the dark irradiance is much more intense than the peak intensity of the soliton beam: $|U| \ll 1$. The part of Eq. (12) that accounts for the normalized index variation δn^* is

$$\delta n^* = -N^2\frac{1}{|U|^2+1}. \qquad (13)$$

Leaving out the constant part of the index modulation, the above approximation implies that $\delta n^* \approx N^2|U|^2$, leading to

$$i\frac{\partial U}{\partial Z} + \frac{1}{2}\frac{\partial^2 U}{\partial X^2} + N^2|U|^2 U = 0. \qquad (14)$$

This is the well-known nonlinear Schrödinger equation, which again exhibits soliton solutions. It has been studied thoroughly (see, for instance, Ref. [20]) and it exhibits well-defined solutions for the small positive integer values of N, which is called the soliton order.

The linear dependence of δn^* upon $|U|^2$ shows that under the conditions detailed above, the steady-state photorefractive effect is similar to the Kerr effect, apart from its much slower response time. The ability to generate spatial

photorefractive solitons is therefore expected and confirmed by the above analysis. Furthermore, Eq. (13) shows that the steady-state photorefractive effect behaves, in certain conditions, like a saturated Kerr effect whose coefficient N^2 can be controlled externally with, for instance, an applied voltage. In the next section, we will show that this has great influence on the temporal behavior of the soliton beams.

III. TEMPORAL ANALYSIS

A. Partial steady-state and space-charge field equation

The temporal behavior of the band-transport model is governed by Eqs. (1a) and (1c). Equation (1a) describes the process of charge generation and recombination. It gives the characteristic carriers recombination time $1/\xi n_e$. Equations (1c) and (1e) express the current distribution continuity and give the dielectric relaxation time $\varepsilon_0 \varepsilon_r / e \mu n_e$, which is the time needed for a photorefractive grating to build up. Therefore, the ratio of the characteristic relaxation time of the donor density to that of the current density is $\delta = \mu e / \varepsilon_0 \varepsilon_r \xi$. In typical photorefractive materials, $\delta \ll 1$. For instance, its maximum value is 2×10^{-4} in LiNbO$_3$, 1×10^{-2} in BaTiO$_3$ [14], and 5×10^{-3} in BSO [21]. This implies that the charge density reaches its steady state much before the current distribution, as confirmed by Yeh [17].

Therefore, after a time longer than the charge recombination characteristic time, Eq. (1a) can be considered as a steady state. The set of equations (15) describes this partially steady band-transport model reduced to one dimension x,

$$0 = (\beta + s I_{\text{em}})(N_D - N_D^+) - \xi n_e N_D^+, \quad (15a)$$

$$\frac{\partial}{\partial x}(\varepsilon_0 \varepsilon_r E) = \rho, \quad (15b)$$

$$\frac{\partial J}{\partial x} + \frac{\partial \rho}{\partial t} = 0, \quad (15c)$$

$$\rho = e(N_D^+ - N_A - n_e), \quad (15d)$$

$$J = e \mu n_e E + \mu \kappa_B T \frac{\partial n_e}{\partial x} + \beta_{\text{ph}}(N_D - N_D^+) I_{\text{em}}. \quad (15e)$$

With no more approximations than those detailed in the above steady-state study, the set of equations (15) can be reduced to a partial differential equation on space and time linking the generalized light power density I to the generalized space charge field E_τ,

$$e \mu \frac{\partial(I E_\tau)}{\partial x} + \kappa_B T \mu \frac{\partial^2 I}{\partial x^2} + \varepsilon_0 \varepsilon_r \frac{I_0}{n_0} \frac{\partial^2 E_\tau}{\partial t \partial x} - e \frac{\partial I}{\partial t} = 0. \quad (16)$$

Solving the partial differential equation (16) requires the accurate definition of the boundary and initial conditions for both I and E_τ. Its solution thus depends on the precise experimental conditions.

Assuming that the light beam has been present for a time considered as infinite, an external electric field E_{ext} is applied to the crystal at $t = 0$. E_τ and I are then assumed to be stable and to reach the steady state described by Eq. (6). As previously defined, the beam extent is considered to be small with respect to the crystal width and its effect is assumed to be limited to its vicinity.

The initial condition for $t = 0$ is not straightforward. Indeed, because of the photorefractive memory effect, the initial state of the refractive index pattern and thus of the space-charge field depend on the crystal history. Therefore, we will propose an incomplete general solution and analyze it for three different assumptions on the space-charge-field initial state.

B. General WPE and its solutions

1. Time-dependent wave propagation equation

Assuming that the light power density varies slowly enough with time so that its last term can be neglected, Eq. (16) can be analytically solved and yields the expression of the generalized space charge field E_τ as a function of I,

$$E_\tau = E_0 \exp\left(-\frac{e \mu}{\varepsilon_0 \varepsilon_r} \frac{n_0}{I_0} It\right) + \left[1 - \exp\left(-\frac{e \mu}{\varepsilon_0 \varepsilon_r} \frac{n_0}{I_0} It\right)\right]$$
$$\times \left((E_{\text{ext}} + E_{\text{ph}})\frac{I_d}{I} - \frac{\kappa_B T}{e} \frac{I'}{I}\right). \quad (17)$$

E_0, the space-charge-field initial state, depends on the space variable x.

In Eq. (17) and in all that derive from it, the exponential terms that describe the time response of the space-charge field depend on the intensity I. It is important to notice that I is the value of the local generalized optical power density [see below Eq. (3) for its precise definition]. It depends on the transverse spatial coordinate x, as does E_τ. This implies that the space-charge-field buildup time constant depends on the transverse spatial coordinate and is, in particular, shorter where the optical power density is larger.

The space-charge field E_τ induces a refractive index variation given by (8) that affects the wave propagation according to (7). The wave propagation equation (18) can thus be derived from (17) using Eqs. (7) and (8),

$$i \frac{\partial U}{\partial Z} + \frac{1}{2} \frac{\partial^2 U}{\partial X^2} - \left[1 - \exp\left(-\frac{I_d(1 + |U|^2)t}{\Sigma}\right)\right]\left(N^2 - D \frac{\partial |U|^2}{\partial X}\right)$$
$$\times \frac{U}{1 + |U|^2} - E_N(X, Z)\exp\left(-\frac{I_d(1 + |U|^2)t}{\Sigma}\right) U = 0. \quad (18)$$

$\Sigma = (\varepsilon_0 \varepsilon_r / e \mu)(I_0/n_0)$ is an energy density determined by the crystal physical parameters. It is characteristic of the relaxation of the self-focusing process. It is a very intimate characteristic of the crystal. We shall choose its value so as to fit our experimental observations ($\Sigma/I_d = 10$ s, see Sec. V below).

The last two terms, divided by U, represent the normalized generalized space-charge field: it is of prime importance to know the spatial and time dependence of this quantity. $E_N(X, Z)$ is the initial normalized generalized space-charge field. As stated above, its value cannot be defined by the general study, for it depends on the crystal history. In the following, three typical cases are analyzed in details.
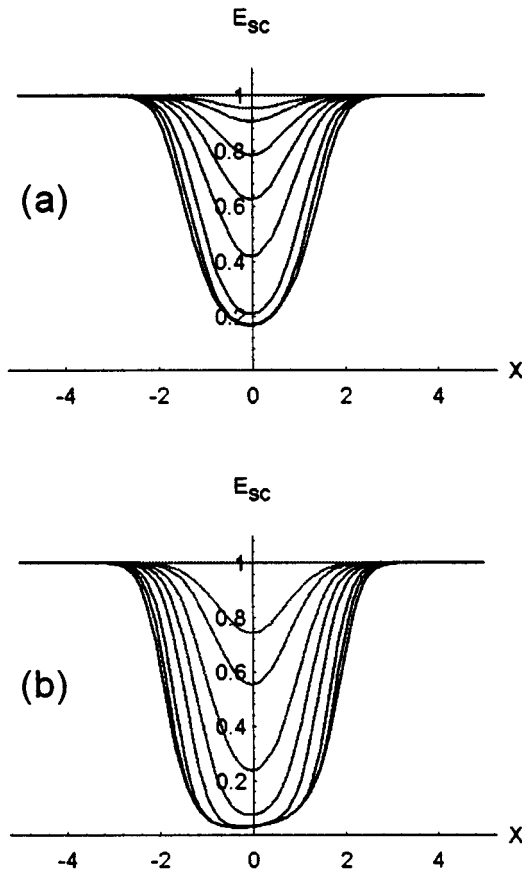
FIG. 1. Normalized space-charge field for t/T_e $=0,0.1,0.2,0.5,1,2,5,10,\infty$ from top to bottom, for $N^2=1$ and $D=10^{-2}$. (a) The soliton beam is five times more powerful than the dark irradiance. (b) The soliton beam is 30 times more powerful than the dark irradiance.

2. Initial state: Uniform space-charge field

The space-charge-field initial pattern is here assumed to be uniform. This assumption cannot be physically accurate for a beam exists prior to the sudden application of the external field. However, it is meaningful when charge diffusion can be neglected, even if no external electric field is applied, and in the absence of any photovoltaic effect. This is true, in particular, for a $Bi_{12}TiO_{20}$ crystal. This means that, before the electric field is applied, the crystal is a linear medium.

Under these conditions, the wave propagation is described by Eq. (18), where

$$E_N(X,Z)=N^2. \qquad (19)$$

Using $N^2=1$ and $D=10^{-2}$, we meet the above requirements. In Fig. 1 the time-dependent normalized value of the space-charge field is shown against the normalized transverse direction X for a Gaussian beam profile and for two ratios of soliton beam peak intensity over dark irradiance: 5 and 30, respectively.

Figure 1 evidences the time behavior of the saturation mechanism of the photorefractive effect. On the one hand, for a not too powerful beam, the photorefractive effect does not saturate and can be considered as quasilocal. The final shape of the space-charge field or refractive index profile
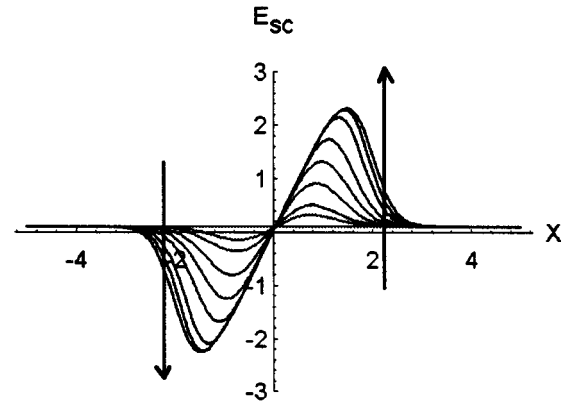

FIG. 2. Normalized space-charge field for t/T_e $=0,0.1,0.2,0.5,1,2,5,10,\infty$, the order being shown by the arrows for a soliton beam 30 times more powerful than the dark irradiance. Here $N^2=10^{-2}$ and $D=1$: diffusion dominates.

remains roughly Gaussian. On the other hand, if the beam is much more powerful than the dark irradiance, then the photorefractive effect saturates. The final shape is no longer Gaussian but resembles a clipped Gaussian. The interesting part is that, during the slow process of saturation, the refractive index pattern is still Gaussian. This suggests, as presented in Sec. IV, that the soliton beam could be narrower during the transient state than at steady state or that the self-focusing effect could be stronger during the transient state.

Although the uniform initial state cannot be physically reached when diffusion is not neglected, the study of this case is interesting for understanding buildup mechanisms. Figure 2 shows, still for a Gaussian beam, what happens if the diffusion mechanism dominates the other ones ($N^2=10^{-2}$, $D=1$), the beam peak intensity being 30 times the dark irradiance. In that case, the quasilocal part of the photorefractive effect is shown to disappear: self-focusing is no longer achieved.

3. Initial state resulting from diffusion

The initial state of the refractive index pattern is here assumed to be due to the prior existence of the beam and to diffusion mechanism of transport, the photovoltaic effect being neglected. In these conditions, the $E_N(X,Z)$ term in the wave propagation equation (18) becomes

$$E_N(X,Z)=N^2-D\frac{\frac{\partial |U|^2}{\partial X}}{|U|^2+1}. \qquad (20)$$

If the diffusion effect can be neglected by comparison to the drift mechanism created by the applied electric field, then the initial state can be considered uniform and the study reduces to what has been shown in Fig. 1: the photorefractive effect is quasilocal.

On the contrary, if the diffusion effect dominates the induced drift mechanism, then the applied electric field has no noticeable effect and the refractive index pattern does not undergo any transient state. The final steady state is shown in Fig. 2 for $t=\infty$.
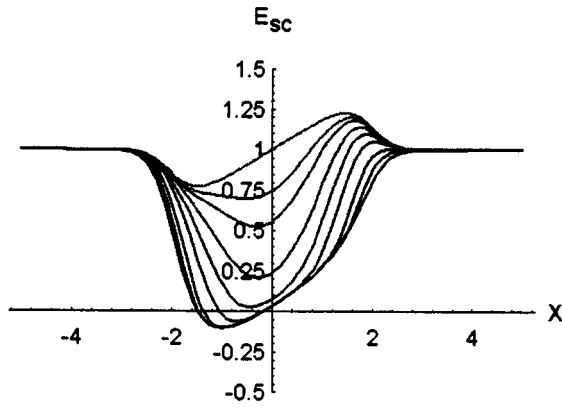
FIG. 3. Normalized space-charge field for t/T_e $=0,0.1,0.2,0.5,1,2,5,10,\infty$ from top to bottom for a soliton beam 30 times more powerful than the dark irradiance. $N^2=1$ and $D=10^{-1}$.

4. Initial state resulting from both diffusion and the photovoltaic effect

The initial state is here considered to result from the prior existence of a beam in a generic photorefractive material where we consider the two mechanisms of transport that remain in the absence of any external field: diffusion and photovoltaic. The term $E_N(X,Z)$ in the wave propagation equation (18) becomes

$$E_N(X,Z)=N^2+\frac{N_{ph}^2-D\dfrac{\partial|U|^2}{\partial X}}{|U|^2+1},\qquad(21)$$

where N_{ph}^2 is N^2, in which the electric field is reduced to E_{ph}.

Figure 4 shows the time behavior of the space-charge field if diffusion is neglected ($N^2=1$ and $D=10^{-2}$) and when the quasilocal and nonlocal mechanisms compete ($N^2=1$ and $D=10^{-1}$). The Gaussian beam is 30 times more powerful than the dark irradiance in both cases. Here N_{ph}^2 is considered to be 10 times lower than N^2. Figure 4 does not evidence a different behavior from Figs. 1 and 3. However, it shows that the photovoltaic effect could, if needed, replace the externally applied electric field.

5. Discussion

The time behavior of the space-charge field and thus of the refractive index profile has been analyzed in detail in the
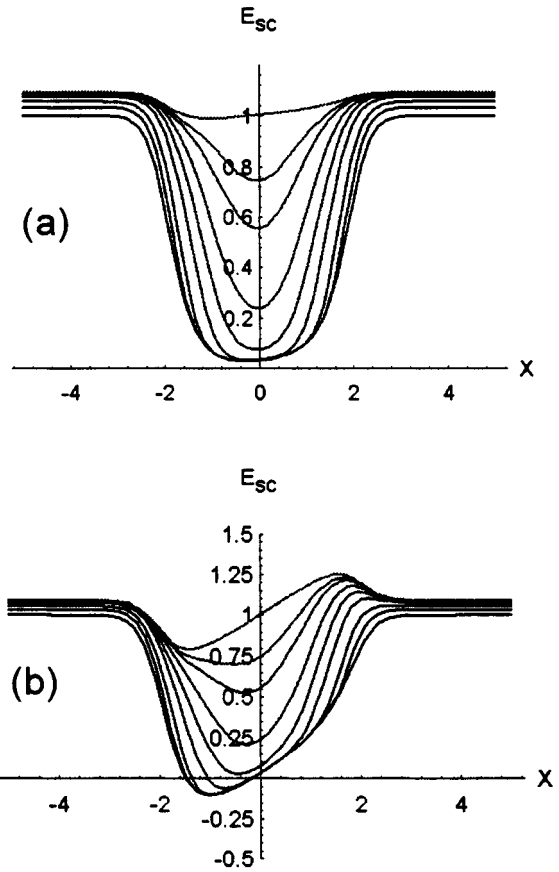
If $N^2=1$ and $D=10^{-1}$, the two mechanisms of diffusion and drift are on the same scale and the quasilocal and nonlocal mechanisms compete. The time behavior of the space-charge field for a Gaussian beam 30 times more powerful than the dark irradiance is shown in Fig. 3. In that case, a strong asymmetry due to the diffusion effect appears in the space-charge field distribution: this suggests that the beam intends to bend towards the deeper part. This may be an explanation to both beam bending and beam fanning phenomena, though this needs to be investigated more thoroughly, like in Ref. [19].

FIG. 4. Normalized space-charge field for t/T_e $=0,0.1,0.2,0.5,1,2,5,10,\infty$ from top to bottom for a soliton beam 30 times more powerful than the dark irradiance. The initial pattern results from the diffusion and photovoltaic effects. (a) $N^2=1$ and $D=10^{-2}$, diffusion plays no significant role; (b) $N^2=1$ and $D=10^{-1}$, diffusion and drift mechanisms compete.

framework of a one-dimensional model. The photorefractive effect has been shown to behave, in certain conditions, like a saturated quasilocal effect. In these cases, bidimensional self-focusing and soliton phenomena are expected and will be shown in Sec. IV.

The saturation phenomenon is evidenced by the flat ''bottom'' of Fig. 1(b). It induces an index pattern that does not match the beam Gaussian shape: the induced waveguide is too wide to effectively guide the beam. Nevertheless, during the transient state, the index profile is closer to that of the beam: a stronger self-focusing, or a narrower soliton beam, is expected. Its time behavior is analyzed in detail below.

The asymmetric shape of Figs. 2, 3, and 4(b), which stems from charge diffusion, suggests that the nonlocal effect could induce a bending of the soliton beam towards the ''deeper'' part of the space-charge field profile. This inference is confirmed by the numerical analysis of Refs. [19,22]. Our analysis suggests that the bending of the beam could be controlled by an external electric field that would dominate the diffusion effect so as to straighten or steer the soliton beam. In a more general manner, it suggests that both the bending and the width of the soliton beam can be controlled by an external electric field.
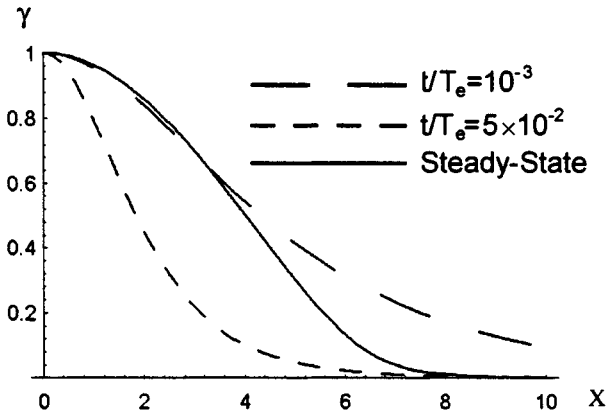
FIG. 5. Time evolution of the normalized soliton profile for $N^2=1$ and $r=100$, typical experimental values.

IV. TIME EVOLUTION OF THE SOLITON PROFILE

The term D of Eq. (18) has been numerically found to induce adiabatic self-deflection in the soliton beam [19]. Therefore, Eq. (18) cannot exhibit strict soliton solutions unless D is considered null. In this section we investigate the time behavior of the soliton profile by neglecting D in Eq. (18), which means that the diffusion mechanism of transport is neglected. Therefore, for simplification purposes and with no loss of generality, we will assume that the initial space-charge field can be considered as uniform. This is particularly the case in the experimental observations on $Bi_{12}TiO_{20}$ presented in Sec. V. The equation that describes the wave propagation under these hypotheses is then Eq. (19).

Let us assume that $U(X,Z,t)$ is a soliton beam: its shape does not change throughout the propagation. It can therefore be expressed as

$$U(X,Z,t)=\sqrt{r}\,\gamma(X,t)e^{i\nu Z},\qquad(22)$$

in which r is the ratio of the soliton beam peak intensity over the dark irradiance, ν is the propagation constant, which will be determined later, and γ is the normalized soliton profile bounded between 0 and 1 [$\gamma(0)=1$, $\gamma(\infty)=0$].

Integrating Eq. (19) using (22) and the above boundary conditions, an analytical expression of ν can be found:

$$\nu=-\frac{N^2}{r}\ln(1+r)+\frac{N^2}{r}\left[\mathrm{Ei}\left(-\frac{I_dt}{\Sigma}(1+r)\right)-\mathrm{Ei}\left(-\frac{I_dt}{\Sigma}\right)\right]$$

$$+\frac{\Sigma}{I_dtr}[e^{-(I_dt/\Sigma)(1+r)}-e^{-I_dt/\Sigma}].\qquad(23)$$

Here Ei is an exponential integral function defined by $\mathrm{Ei}(z)=-\int_{-z}^{\infty}(e^{-t}/t)\partial t$.

The soliton profile γ is then given by the differential equation on X (24), derived from (19) and (22),

$$-2\nu\gamma+\gamma''-(1-e^{-(I_dt/\Sigma)(1+r\gamma^2)})\left(2N^2\frac{\gamma}{1+r\gamma^2}\right)$$

$$-2\gamma e^{-(I_dt/\Sigma)(1+r\gamma^2)}=0,\qquad(24)$$

where γ'' is the second derivative of γ with respect to X. This equation can be numerically integrated by conventional
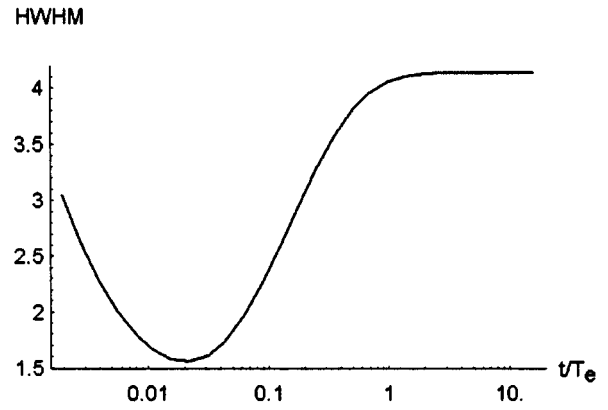

FIG. 6. Time evolution of the normalized soliton HWHM for the same conditions as in Fig. 5.

methods. Figure 5 shows three examples of the time evolution of the normalized soliton profile towards the so-called screening soliton [11], reached at steady state. The numerical values taken for Fig. 5 are $N^2=1$ and $r=100$, typical of our experiments. The high value for r explains the large screening soliton diameter (or low self-focusing power). Nevertheless, Fig. 5 shows that, during transient state, the self-focusing power is stronger.

Such calculations allow us to compute the time evolution of the soliton half-width at half maximum (HWHM) shown in Fig. 6. The time normalization factor T_e used in Figs. 5–8 is $T_e=\Sigma/I_d$. For high saturation values (i.e., $r>1$), the soliton HWHM reaches a minimum during transient state. This is the so-called quasisteady soliton [10].

Figure 7 shows the diameters of the screening soliton (plain curve) and of the quasisteady soliton (dotted curve). It shows that, as suggested in Refs. [1,2], the diameter of the quasisteady soliton does not depend on r as long as it is larger than 1. On the contrary, for small values of r, the soliton HWHM minimum is reached at steady state, since the photorefractive process does not saturate anymore. The quasisteady soliton and the screening soliton thus merge for small values of r and their common spatial behavior is that of the Kerr soliton.

Figure 7 summarizes the main results of the above temporal analysis. It confirms the existence of photorefractive
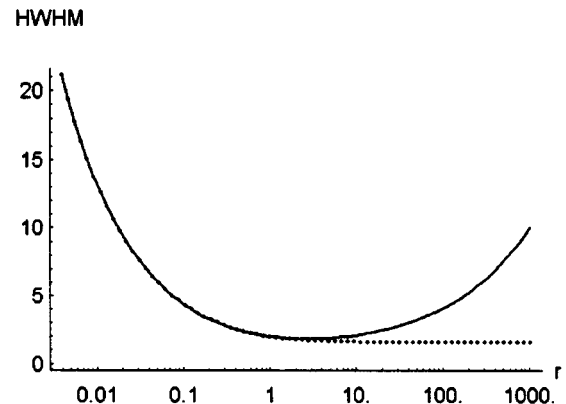

FIG. 7. Soliton HWHM as a function of r: solid line, the screening soliton (steady state); dotted line, the quasisteady soliton (minimum HWHM reached during transient state).
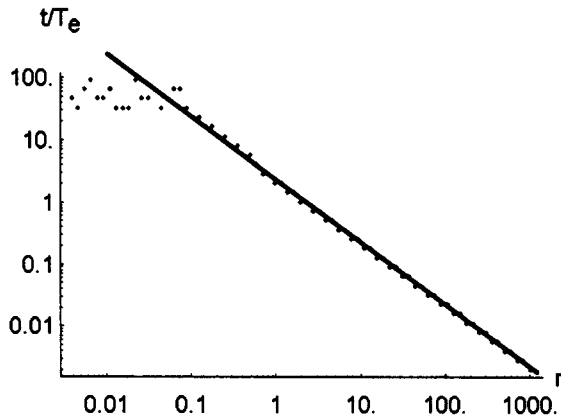
FIG. 8. Time to reach the quasisteady soliton state, as a function of the peak power to dark irradiance ratio r. Each point shows one calculated time, whereas the solid line is a mere guide to the eye. The points off the line are due to the lack of computer precision. The curve linearity suggests that $r*(t/T_e)$ is a constant.

quasisteady solitons and retrieves their main properties, found previously by analytical means in Refs. [1,2], such as their independence upon the absolute light intensity and on its ratio to dark irradiance, provided it is larger than unity. Furthermore, it confirms the existence of photorefractive screening solitons predicted by Ref. [11].

Figure 8 shows the time needed to reach the quasisteady soliton as a function of r. For small r, this time tends to infinity. This explains the points off the line, due to the lack of computation precision. The curve linearity shows that this response time is inversely proportional to a power of r defined by the slope of the line. For $N^2 = 1$, it can be deduced from Fig. 8 that $r*(t/T_e)$ is a constant. This suggests that the response time can be as short as desired, provided r can be increased enough. However, further analysis of the soliton HWHM time behavior seems to show that the lifetime of the quasisteady soliton is roughly proportional to its time response, which may be a limit to the use of short-response-time quasisteady soliton.

V. EXPERIMENTAL RESULTS

In order to have a first validation of the previously detailed theoretical results, we have experimentally investigated the photorefractive self-focusing with the experimental setup shown in Fig. 9. A 4 mW polarized HeNe laser is focused onto a $Bi_{12}TiO_{20}$ crystal, so that its waist is around 30 μm. Its polarization is set to be parallel to the electric field applied to the $Bi_{12}TiO_{20}$ crystal. Its intensity is reduced with two rotating polarizers so that its power density on the entrance face of the crystal is of the order of the mW/cm^2 level. The crystal is 3.17 mm in length and the electric field is applied onto the 4.17-mm-long transverse dimension. The remaining dimension is 4 mm in length. A 5 mW, 670 nm diode laser is used to provide a uniform background light to the crystal so as to simulate the effects of the dark irradiance. An interference bandpass filter tuned to the 633-nm laser wavelength is used to separate the soliton beam issued from the HeNe laser from the 670 nm light that is channeled into the self-induced waveguide.
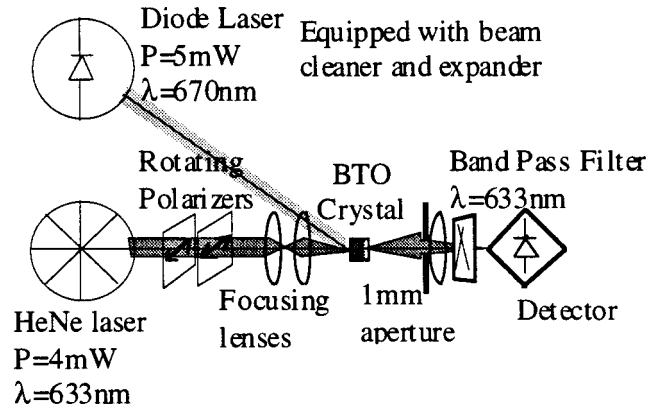

FIG. 9. Experimental setup for the observation of the soliton phenomenon in $Bi_{12}TiO_{20}$.

A 1 mm aperture is placed at 12 cm away from the exit face of the crystal. The light transmitted through it is gathered onto a photodiode. This is a spatial filtering technique that allows, as shown below, one to directly measure the output beam diameter.

Let d be the radius of the aperture and L its distance to the crystal. The wave surface on the exit face of the crystal is assumed to be plane, which is precisely true if a soliton beam is generated [3]. Though it is not strictly needed, we will assume the wave profile to be Gaussian. This hypothesis is used to help carry out the calculations, but the general diffraction properties of light are so that the method remains valid for profiles that are not strictly Gaussian.

Using the complex curvature method, it is straightforward to show that the beam profile on the aperture plane is, when normalized to 1,

$$I(x) = \frac{e^{-(x/W_1^2)^2}}{W_1^2} \quad \text{with} \quad W_1 = \frac{\lambda L}{\pi W_0}.$$

Here W_0 is the radius of the beam on the exit face of the crystal. It can then be readily shown that the total normalized light intensity transmitted through the aperture is

$$I_a = \pi \left(1 - \frac{1}{e^{(d\pi W_0/\lambda L)^2}} \right).$$

On our experimental apparatus, $\lambda = 633$ nm, $L = 125$ mm, and $d = 0.5$ mm. Figure 10 shows that in that case, I_a is quasiproportional to W_0 as long as it is less than 100 μm. Therefore this spatial filtering technique allows, by measuring I_a, to have a real time measurement of the output beam diameter.

Figure 11 shows the output beam diameter against time when the externally applied voltage is suddenly switched on and then switched off after 40 s. The beam undergoes a temporary self-focusing lasting a few seconds before relaxing to a less focused state. This is consistent with the above theory and fits with Fig. 6, as well as with the numerically evaluated beam profile time behavior from Ref. [15].

Figure 12 shows the influence of photorefractive saturation upon both the transient and the steady state. The relative output diameter is plotted against the ratio of the beam peak
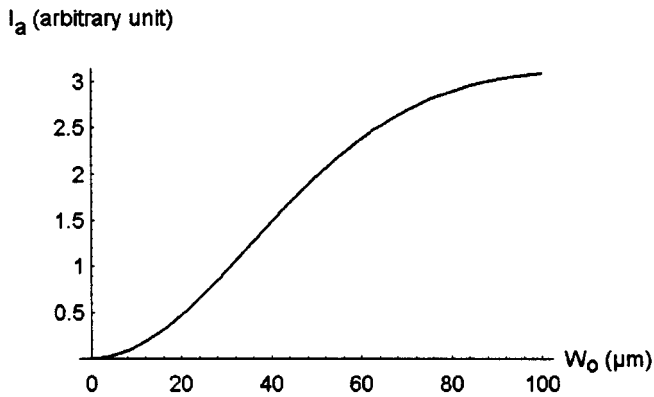
FIG. 10. Transmitted intensity through the aperture as a function of the output beam waist.

power over the dark irradiance. A relative output diameter of 1 means that the beam has propagated with no change of shape: a soliton beam has been achieved. Below 1, it means that the beam overfocuses: the nonlinearity is too strong to generate a first-order soliton. A value of 1.05 means that no effect can be noticed. Indeed, it is the value reached with no electric field applied, the material then being considered linear.

It should be noticed, though, that the physical phenomenon measured in Figs. 11 and 12 is not exactly what is plotted in Figs. 6 and 7. Indeed, the former show the ratio of the output diameter over the input one, which could be called the self-focusing power, whereas the latter show the soliton diameter, which is assumed to exist. Though these phenomena result from the same basic physical effects, they are not strictly identical. Therefore these two pairs of curves, though they are quantitative, cannot be strictly compared quantitatively.

The solid curve in Fig. 12 corresponds to the steady-state experimental results. It is in good agreement with Fig. 7 and with Ref. [18], along with the experimental results presented in Ref. [23]. The dotted curve of Fig. 12 shows the minimum
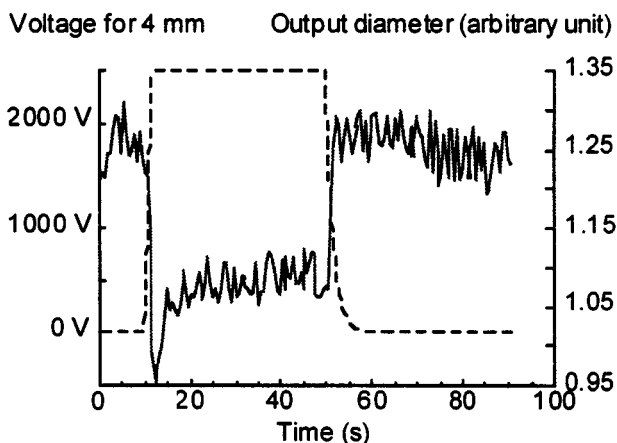

FIG. 11. Measured output beam waist using the spatial filtering technique, for an input beam waist of 30 μm. The dotted lines show the applied voltage (to a 4-mm-wide crystal). The output beam waist, shown by the solid line, undergoes temporary self-focusing and relaxes to a self-focused state until the voltage is switched off.
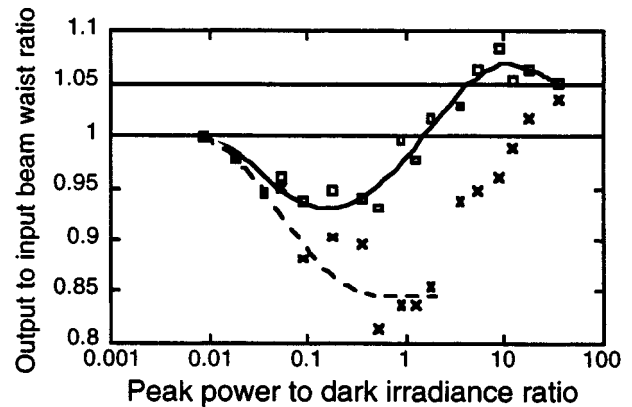

FIG. 12. Measured ratio of the output beam waist over the input beam waist versus peak power to dark irradiance ratio, for an input beam waist of 30 μm. The squares show the raw measurements of the steady-state ratio, the solid line being a simple guide. The crosses show the measured minimum transient ratio, the dotted line showing the expected and explained behavior.

diameter achieved during transient state. It joins the solid curve for small values of the peak intensity to dark irradiance ratio: if the beam peak local intensity is lower than that of the dark irradiance, the photorefractive effect does not saturate and the minimum achieved diameter is that of a steady state. It is not quite clear why the same thing happens for large values of the intensity ratio. Nevertheless, this is probably due to the fact that, as Fig. 8 suggests, the transient state is too short in time for our measurement apparatus to catch it. If this assumption is correct, our experimental results are in good agreement with Fig. 7 and with the experimental quasi-steady-state soliton results of Ref. [24]: they all suggest that the quasi-steady-state soliton does not depend on r, provided it is large enough.

Aside from this latter point, the experimental results presented here are in good agreement with the above theoretical study. Further experimental investigations aimed at characterizing the steady-state and transient self-focusing as well as spatial soliton beams on other and better quality crystals are on the way.

CONCLUSION

We have investigated the temporal behavior of the photorefractive effect, on the basis of a bidimensional band-transport model. We have shown that the photovoltaic effect and the drift mechanism of charge transport could be thought of as similar and their effects are additive. We have derived a time-dependent wave propagation equation in generic photorefractive media, which describes the propagation of any light beam, provided that its transverse profile is smooth enough so that the slow variation approximation is valid. This equation exhibits bright spatial soliton solutions whose evolution against time has been investigated. It describes successfully the behavior of the three previously found bright soliton types, namely, the quasisteady, steady-state, and photovoltaic solitons, whose properties are consistent with previous theoretical studies. In particular, the quasi-steady soliton diameter is found to be independent of the ratio of the light peak intensity over the dark irradiance, pro-

vided it is larger than unity. Furthermore, it has been intimated that the quasisteady soliton state could be reached as rapidly as desired, provided the above intensity ratio r can be raised sufficiently. In addition, we have suggested that the diffusion process could induce a beam bending, which might be controlled, along with the soliton beam diameter, by an externally applied electric field. Finally, an experimental validation of these theoretical considerations has been provided, which confirms the various conclusions stated above.

[1] M. Segev, B. Crosignani, and A. Yariv, Phys. Rev. Lett. **68**, 923 (1992).

[2] B. Crosignani, M. Segev, D. Engin, P. Di Porto, A. Yariv, and G. Salamo, J. Opt. Soc. Am. B **10**, 446 (1993).

[3] M. Segev, B. Crosignani, P. Di Porto, G. C. Duree, G. Salamo, and E. Sharp, Opt. Lett. **19**, 1296 (1994).

[4] D. N. Chistodoulides and M. I. Carvalho, Opt. Lett. **19**, 1714 (1994).

[5] M. D. Iturbe Castillo, P. A. Marquez Aguilar, J. J. Sanchez Mandragon, S. Stepanov, and V. Vysloukh, Appl. Phys. Lett. **64**, 408 (1994).

[6] G. C. Duree, J. L. Schultz, G. J. Salamo, M. Segev, A. Yariv, B. Crosignani, P. Di Porto, E. J. Sharp, and R. R. Neurgaonkar, Phys. Rev. Lett. **71**, 533 (1993).

[7] M. F. Shih, M. Segev, G. C. Valley, G. Salamo, B. Crosignani, and P. Di Porto, Electron. Lett. **31**, 826 (1995).

[8] M. T. Taya, M. C. Bashaw, M. Segev, and G. C. Valley, Phys. Rev. A **52**, 3095 (1995).

[9] G. C. Duree, G. Salamo, M. Segev, A. Yariv, B. Crosignani, P. Di Porto, and E. Sharp, Opt. Lett. **19**, 1195 (1994).

[10] M. Morin, G. Duree, G. Salamo, and M. Segev, Opt. Lett. **20**, 2066 (1995).

[11] M. Segev, G. C. Valley, B. Crosignani, P. Di Porto, and A. Yariv, Phys. Rev. Lett. **73**, 3211 (1994).

[12] G. C. Valley, M. Segev, B. Crosignani, A. Yariv, M. M. Fejer,

and M. C. Bashaw, Phys. Rev. A **50**, 4457 (1994).

[13] S. Maneuf, R. Desailly, and C. Froehly, Opt. Commun. **65**, 193 (1988).

[14] A. A. Zozulya and D. Z. Anderson, Phys. Rev. A **51**, 1520 (1995).

[15] A. A. Zozulya and D. Z. Anderson, Opt. Lett. **20**, 837 (1995).

[16] N. V. Kukhtarev, V. B. Markov, S. G. Odulov, M. S. Soskin, and V. L. Vinetskii, Ferroelectrics **22**, 949 (1979).

[17] P. Yeh, *Introduction to Photorefractive Nonlinear Optics* (Wiley-Interscience, New York, 1993).

[18] D. N. Christodoulides and M. I. Carvalho, J. Opt. Soc. Am. B **12**, 1628 (1995).

[19] S. R. Singh and D. N. Christodoulides, Opt. Commun. **118**, 569 (1995).

[20] G. P. Agrawal, *Nonlinear Fiber Optic* (Academic, London, 1989).

[21] G. Lesaux, G. Roosen, and A. Brun, Opt. Commun. **56**, 374 (1986).

[22] M. I. Carvalho, S. R. Singh, and D. N. Christodoulides, Opt. Commun. **120**, 311 (1995).

[23] K. Kos, H. Meng, G. Salamo, M. Shih, M. Segev, and G. C. Valley, Phys. Rev. E **53**, R4330 (1996).

[24] G. C. Duree, M. Morin, G. Salamo, M. Segev, B. Crosignani, P. Di Porto, E. Sharp, and A. Yariv, Phys. Rev. Lett. **74**, 1978 (1995).